



HAL
open science

Vasa nervorum angiogenesis in prostate cancer with perineural invasion.

Nicolae Ghinea, Blaise Robin, Christophe Pichon, Renaud Leclere, André Nicolas, Caroline Chnecker, Jean-François Côté, Bertrand Guillonneau, Aurelian Radu

► **To cite this version:**

Nicolae Ghinea, Blaise Robin, Christophe Pichon, Renaud Leclere, André Nicolas, et al.. Vasa nervorum angiogenesis in prostate cancer with perineural invasion.. *Prostate*, 2019, 79 (6), pp.640-646. 10.1002/pros.23771 . hal-02179478

HAL Id: hal-02179478

<https://hal.sorbonne-universite.fr/hal-02179478>

Submitted on 10 Jul 2019

HAL is a multi-disciplinary open access archive for the deposit and dissemination of scientific research documents, whether they are published or not. The documents may come from teaching and research institutions in France or abroad, or from public or private research centers.

L'archive ouverte pluridisciplinaire **HAL**, est destinée au dépôt et à la diffusion de documents scientifiques de niveau recherche, publiés ou non, émanant des établissements d'enseignement et de recherche français ou étrangers, des laboratoires publics ou privés.

1 **VASA NERVORUM ANGIOGENESIS IN PROSTATE CANCER WITH PERINEURAL**
2 **INVASION**

3 Nicolae Ghinea^{1*}, Blaise Robin¹, Christophe Pichon¹, Renaud Leclere², André Nicolas²,
4 Caroline Chnecker³, Jean-François Côté⁴, Bertrand Guillonneau⁵, Aurelian Radu⁶

5 ¹ Institut Curie, Université de recherche Paris-Sciences-et-Lettres, Département
6 Recherche Translationnelle, Equipe Angiogenèse tumorale, Paris, France

7 ² Hôpital Curie, Université de recherche Paris-Sciences-et-Lettres, Pôle de médecine
8 diagnostique et théranostique, Paris, France

9 ³ Hôpital Lariboisière, Service d'Anatomie et de Cytologie Pathologiques, Paris, France

10 ⁴ Hôpital Pitié-Salpêtrière, Service d'Anatomie et de Cytologie Pathologiques, Paris,
11 France

12 ⁵ Hôpital Diaconesses-Croix St Simon, Service Urologie, Paris, France

13 ⁶ Icahn School of Medicine at Mount Sinai, Department of Cell, Developmental and
14 Regenerative Biology, One Gustave L Levy Place, New York, NY, USA

15
16 ***Corresponding Author:**

17 Nicolae Ghinea, Ph.D

18 Université de Recherche Paris Sciences et Lettres, Institut Curie, Département
19 Recherche Translationnelle, Equipe Angiogenèse tumorale, 26 rue d'Ulm, 75248-Paris,
20 France

21 E-mail: nicolae.ghinea@curie.fr; Phone: +33 1 5624 6594

22
23 **Running title:**

24 **VASA NERVORUM ANGIOGENESIS IN PROSTATE CANCER**

25 **Keywords**

26 Angiogenesis, CD34, D2-40, FGF-2, FSHR, locally advanced prostate cancer,
27 neoangiogenic markers, perineural invasion, podoplanin, vasa nervorum, VEGF,
28 VEGFR-2, vascular remodeling

29 **Abstract**

30 **Background.** Perineural invasion (PNI) is generally accepted as a major route of cancer
31 dissemination in malignancies associated with highly innervated organs. However, the
32 effect of cancer cells on vasa nervorum remains unknown. We studied this effect in
33 locally advanced prostate cancer, a high-risk feature associated with approximately 20 %
34 of prostate cancer specific mortality.

35 **Methods.** We used immunohistochemistry for CD34, fibroblast growth factor-2 (FGF-2),
36 FSHR, podoplanin, vascular endothelial growth factor (VEGF), and VEGFR-2 as well as
37 histochemical methods to examine the vasa nervorum of nerves invaded by cancer cells
38 in tissue samples from 85 patients.

39 **Results.** The percentage of the nerve area occupied by CD34-positive vasa nervorum
40 endothelial cells in nerves with PNI was much higher than in nerves without PNI ($7.3 \pm$
41 1.2 versus 1.9 ± 0.4 ; $p < 0.001$ and 5.8 ± 0.6 versus 1.23 ± 0.8 ; $p < 0.001$ in pT3a and pT3b
42 prostate cancer specimens, respectively). In 19/85 of the patients the CD34-positive vasa
43 nervorum microvessels have a thick basement membrane, similar to the vessels in
44 diabetic microangiopathy. This subendothelial layer contains collagen fibers. Vasa
45 nervorum endothelia and Schwann cells express FGF-2 (nuclear localization) and FSHR
46 (plasma membrane and cytoplasmic staining). Prostate cancer cells invading nerves
47 express VEGF, a critical cytokine in tumor angiogenesis. The vasa nervorum of prostatic
48 nerves with PNI did not express detectable levels of VEGFR-2. No podoplanin-positive
49 lymphatic vessels were seen in nerves.

50 **Conclusion.** In locally advanced prostate cancer, perineural invasion of cancer cells is
51 associated with formation of new endoneurial capillaries and changes of vasa nervorum
52 morphology.

INTRODUCTION

Tumor metastasis is a complex and highly selective process whereby cancer cells leave the primary tumor site and disseminate to other locations¹ via distinct routes involving blood vessels, lymphatic vessels, coelomatic cavities, and migration of cancer cells along nerves². The latter route is encountered frequently in prostate and other cancers (pancreas, colon, rectum, biliary tract, stomach, skin, salivary gland, head and neck)³. Migration of cancer cells in close proximity of the nerve and/or within any of the three layers of the nerve (epineurium, perineurium, and endoneurium) constitutes the perineural invasion process⁴. Secreted neurotrophic factors that form a concentration gradient along nerves^{5,6} may play a pivotal role in perineural invasion⁷. This is the case of the glial-derived growth factor that activates RET-receptor mediated cancer cell chemotaxis, which in turn guides the directional cancer cell migration towards and along the nerves⁸. Nerves not only harbor cancer cells, but they appear to actively promote cancer cell penetration of the nerves⁹ and survival, and decreased apoptosis of the invading cells¹⁰.

Recent studies have demonstrated that perineural invasion results in i) cancer-related axogenesis/neurogenesis¹¹ and ii) cancer cell proliferation and migration^{11,12}. These biological processes are highly dependent on a local supply of oxygen and nutrients provided by blood vessels that accompany the nerves and/or penetrate into the nerves (vasa nervorum). However, basic questions about blood supply for perineural invasion zones remain unanswered. For example, it is not known if the invading cancer cells in human tumors utilize the same strategies as those well documented in animal models of prostate cancer (ex., neovascularization by sprouting angiogenesis from pre-existing endothelial cells in established vessels)¹³. A potential alternative is that perineural invasion develops the ability to progress independently of neovascularization. The answers to these questions should critically impact the potential of new therapeutic

82 approaches to prevent cancer cells from leaving the primary tumor site and disseminate
83 to distant organs.

84 Antibodies for endothelial cell markers (Table 2), were used to study the effect of
85 perineural invasion on vasa nervorum in patients diagnosed with locally advanced
86 prostate cancer. In this type of cancer the tumor cells penetrated through the
87 fibromuscular pseudocapsule covering the prostate gland, but did not spread to lymph
88 nodes or to distant areas (T3-N0-M0, in the TNM staging system¹⁴. We analyzed locally
89 advanced prostate cancer specimens because this type of cancer comprises about 5-
90 10 % of all newly diagnosed prostate cancers and it is associated with approximately
91 20 % of prostate cancer specific mortality¹⁵. Modifications in the morphology of vasa
92 nervorum have been also analyzed by histochemical methods.

94 **MATERIALS AND METHODS**

95 ***Tissue specimens***

96 Paraffin sections of locally advanced prostate cancer tissue fixed in 10% neutral
97 formalin were obtained from the biorepositories of Paris Hospitals Lariboisière (57
98 patients) and Tenon (28 patients) (Table1). The prostate cancer tissues were included in
99 paraffin in the period 2009-2015. Two pathologists (C.C. and J-F.C.) reviewed all cases
100 for the present study. The pathologic stage T3 (pT3) was assigned according to the
101 World Health Organization guidelines¹⁶. Extraprostatic extension (pT3a) was diagnosed if
102 tumor cells were present in the periprostatic soft tissue or penetrated through a
103 fibromuscular pseudocapsule and came out on the other side. The seminal vesicle
104 invasion (pT3b) was defined as tumor tissue present within the fibromuscular wall of the
105 seminal vesicles. All pelvic lymph nodes were evaluated for the presence of metastatic
106 disease. All cases were assigned a Gleason score.

107 The protocol was approved by the institutional ethics committee at each study site.
108 Written informed consent was obtained at the time of surgery from all living donors from
109 whom samples were obtained.
110

111 ***Immunohistochemistry***

112 Paraffin sections (5 μ m) of both pT3a and pT3b tumors were immunolabeled with
113 antibodies directed against several endothelial markers (Table 2). Immunohistochemistry
114 was carried out using an automated immunohistochemical stainer according to the
115 manufacturer's guidelines (Leica Bond RX, Leica Biosystems). Antigen retrieval was
116 conducted by treatment with high temperature at pH 6 or pH 9 (Table 2).

117 118 ***Image and statistical analysis***

119 In our study we have analyzed all the nerves (invaded or not invaded by cancer
120 cells) present on the tissue paraffin sections (the range was 3 – 20 nerve profiles per
121 section). The normal nerve profiles were located at least 500 μ m from the tumor border,
122 outside the prostatic stroma. The nerves with PNI were analyzed inside and outside the
123 prostatic stroma. We have quantitatively determined the density of FSHR-, CD34-, D2-
124 40-positive blood vessels. This was done by counting the number of marker-positive
125 vessels on digital images from whole images of serial sections obtained by using the
126 Philips Digital Ultra-Fast Scanner 1.6 RA and Philips Image Management System 2.2RA,
127 available in Curie Institute. The area occupied by CD34-positive endoneurial endothelial
128 cells was calculated using the formula: % of endoneurial endothelial cells area = Σ pixels
129 of endoneurial endothelial cells area \times 100 / Σ pixels of the nerve area, as previously
130 described¹⁷. The pixel density of the image was measured with the "color deconvolution
131 function" of FIJI software in the range of 0 – 255, where 0 means presence of endothelial
132 cells and 255 means absence. The computations were performed separately for nerve
133 areas in which tumoral invasion was present or absent. The values presented are means
134
135

136 ± standard deviations (SD). Relationships between the vascular expression of CD34 and
137 FSHR, and clinicopathological data were examined by Pearson's correlation coefficient.
138 The statistical significance was evaluated using the 2-tailed t-test.

140 RESULTS

141 *Effect of cancer invasion of nerves on vasa nervorum*

142 In order to obtain reliable results, we had to analyze the effect of PNI on vasa
143 nervorum in nerve-reach prostate areas. Published data indicate that the innervation of
144 prostate is richest in the “capsular” regions, with density of innervation increasing towards
145 the seminal vesicles¹⁸. These areas correspond to the pathological T3a and T3b prostate
146 tumors¹⁶, which we have analyzed in the present study. We noticed the presence of
147 prostate cancer cells along these nerves (Fig. 1A). In the majority of the cases PNI was
148 detected before metastasis, which is the result of dissemination through lymphatic or
149 blood vessels.

150 The presence of cancer cells within any of the three layers of the nerve (i.e.,
151 epineurium, perineurium, and endoneurium) may cause compression and destabilization
152 of vasa nervorum, which should lead to reduced perfusion and hypoxia. Hypoxia, in turn,
153 is known to induce secretion of angiogenic factors involved in prostate cancer
154 progression and metastasis¹⁹. Because the formation of new endoneurial capillaries *in*
155 *vitro* depends on the presence of angiogenic factors²⁰, we have analyzed by
156 immunohistochemistry the expression of two potent angiogenic factors: VEGF and FGF-
157 2. VEGF was present in the cytoplasm of most cancer cells, including those surrounding
158 the nerves (Fig. 1B). FGF-2 was observed in the nuclei of vasa nervorum and Schwann
159 cells, both in nerves that have or do not have perineural invasion (Fig. 1C). A strong
160 FGF-2 staining was also noticed in both tumor and peritumoral endothelial cells (not
161 illustrated). These results suggest that VEGF and FGF-2, via their endothelial receptors,

162 may activate pathways leading to endothelial cell proliferation and new vasa nervorum
163 formation.

164 Angiogenesis of vasa nervorum induced by PNI is expected to lead to increased
165 number of endothelial cells per mm² of nerves. To find out whether this is the case, we
166 determined the percentage of nerve area occupied by endothelial cells, as detected by
167 the endothelial marker CD34²¹. The pictures in Figs. 2A and 2B are representative for the
168 distribution of CD34-positive vasa nervorum of nerves without or without PNI,
169 respectively. A similar pattern was noticed for two other neurotropic cancers, pancreatic
170 cancer and colon cancer (not illustrated).

171 In the pT3a prostate cancer specimens, the percentage of the area occupied by
172 CD34-positive endothelial cells associated to the nerves with PNI was much higher than
173 that in nerves without PNI ($7.3 \pm 1.2\%$ *versus* $1.9 \pm 0.4\%$; $p < 0.001$) (Fig. 2C). In the
174 pT3b prostate cancer specimens, the percentage of the area occupied by CD34-positive
175 endothelial cells associated to the nerves with PNI was also much higher than that in
176 nerves without PNI (5.8 ± 0.6 *versus* 1.23 ± 0.8 ; $p < 0.001$). No significant difference was
177 found between pT3a and pT3b cases ($p = 0.59$). The percentage of the nerve area
178 occupied by CD34-positive endothelial cells in the nerves with PNI correlated with the
179 clinical stage ($r = 0.62$; $p = 0.008$) and with the tumor size ($r = 0.62$; $p = 0.01$).

180 Although it is generally thought that cancer is associated with increased
181 microvessel density in a variety of human cancers, this view is controversial for prostate
182 cancer²². We have determined the CD34-positive vessel density in the prostate in regions
183 of cancer and in the benign peritumoral area. Our results showed that tissue sections
184 without cancer were significantly more vascularized than were tumors ($3.28 \pm 0.5 \%$
185 *versus* $2.01 \pm 0.32\%$; $p = 0.03$).

186 All these results indicate that an angiogenic process occurred for vasa nervorum
187 of cancer invaded nerves.

188 In 19/85 (22%) of patients with pT3 tumors, the vasa nervorum in nerves with
189 perineural invasion had a thick subendothelial layer containing collagen fibers (Fig. 3A),
190 in comparison with non-invaded vasa nervorum) (Fig. 3B). Standard histochemical
191 staining (hematoxylin-eosin-saffron staining, periodic acid-Schiff reaction and Masson's
192 trichrome technique) indicated that in 19/85 (22%) of patients with pT3 tumors, the vasa
193 nervorum in nerves with perineural invasion had a thick subendothelial layer containing
194 collagen fibers, characterized by the absence of pericytes (Fig. 3).

195 The vasa nervorum of prostatic nerves with PNI did not express detectable levels
196 of VEGFR-2. No podoplanin-positive lymphatic vessels were seen in nerves.

197 Work from our laboratory showed that FSHR is expressed by the tumor
198 endothelial cells, most frequently at the periphery of prostate cancer tissue²³. However,
199 no information was available for the vascular FSHR expression in zones of perineural
200 invasion in locally advanced prostate cancer. The density of FSHR-positive vasa
201 nervorum (number of vessels/mm² of nerve tissue) of nerves with perineural invasion was
202 not significantly different from that of nerves without perineural invasion (47.8 ± 12.5
203 *versus* 46.8 ± 10.4 ; $p = 0.9$). The density of FSHR-positive vasa nervorum correlated with
204 both the final Gleason score ($r = 0.48$; $p = 0.02$) and tumor size ($r = 0.69$; $p = 0.003$). We
205 noticed also intense FSHR staining of Schwann cells in all nerve ganglia and nerve fibers
206 in peripheral areas affected by perineural invasion (Fig. 3D). No immunohistochemical
207 signal was obtained by using an irrelevant mouse antibody of the same IgG2a subtype as
208 FSHRA02 (not illustrated). In benign peritumoral tissues of cancer patients the nerves
209 show also intense FSHR staining of Schwann cells and vasa nervorum at all analyzed
210 Gleason scores (5-9). On a radical prostatectomy specimen obtained for a non tumor
211 related disease, the majority of nerves and their associated vessels in the peripheral
212 areas of the prostate do not express FSHR (not illustrated). The absence of staining in
213 nerves and blood vessels was also noticed in a nerve ganglion in the peripheral zone.

214 The above results suggest that perineural invasion by prostate cancer cells could
215 have important effects on the nerve microvessels by inducing angiogenesis and vascular
216 remodeling.

218 **DISCUSSION**

219 Our study indicates that an angiogenic process occurs at the level of vasa
220 nervorum of cancer invaded nerves, in comparison with the nerves that are not invaded.
221 The increased blood supply is expected to facilitate further growth and invasion of tumor
222 cells along the nerves, and progression of the disease.

223 The density of blood vessels in the cancer invaded nerves is higher than in the
224 non-invaded nerves. This indicates that the angiogenic process in the cancer invaded
225 nerves is caused by the proximity of both nerve and tumor cells. Angiogenesis could be
226 induced by angiogenic factors released by the tumor cells, and the release can be
227 induced by the adjacent nerves, or vice-versa. Angiogenesis was shown to occur in
228 nerve cell grafts and at spinal cord lesions during peripheral nerve regeneration, and can
229 be triggered by physiological tasks that increase neural function and synaptic activity^{24,25}.
230 It is possible that such increased neural function is induced by the tumor cells that invade
231 the nerves.

232 In mouse models of prostate cancer, noradrenaline generated by nerves induces
233 angiogenesis by activating adrenergic receptors on the endothelial cells, which in turn
234 alter the endothelial cell metabolism²⁶. Therapies attempting to starve the tumor by
235 inhibiting angiogenesis had limited long term therapeutic benefit in various cancers,
236 including that of the prostate²⁷, most likely due to resistance mechanisms²⁸. Co-targeting
237 angiogenesis, neural signals and/or endothelial cell metabolism may provide a
238 multipronged therapeutic approach to inhibit cancer invasion via the nerves²⁶.

239 Analysis of the morphology of blood vessels in nerves with perineural invasion
240 indicated that in 22% of patients with locally advanced prostate cancer the vasa

241 nervorum had a thick collagenous subendothelial layer in comparison with normal vasa
242 nervorum. Another characteristic of these microvessels is the absence of pericytes
243 associated with the capillaries and postcapillary venules. Pericytes are distinctive
244 regulators of angiogenesis and are thought to provide vessel stability and control of
245 endothelial proliferation²⁹. The modified walls of these vessels could constitute an
246 adaptation to ensure constant blood flow. The walls of normal vessels constantly adjust
247 the vessel diameter to adapt to the metabolic needs of the tissue. The thick walls and the
248 absence of contractile cells indicate that this process does not occur in the modified
249 vessels, ensuring a constant, possibly maximal blood flow.

250 Thickening of the capillary basement membrane is a hallmark of diabetic
251 microangiopathy, and may lead to occlusive angiopathy and to tissue hypoxia and
252 damage³⁰.

253 The vasa nervorum of prostatic nerves with perineural invasion do not express
254 detectable levels of VEGFR-2. This observation indicates that the angiogenic process
255 induced by perineural invasion could not involve VEGF/VEGFR-2 /signaling.

256 The data were obtained from locally advanced prostate cancer, which is
257 associated with approximately 20% of prostate cancer specific mortality. Most likely the
258 data have a more general significance, based on the fact that migration of cancer cells
259 along the nerves is encountered in other cancers in highly enervated organs (pancreas,
260 colon, rectum, biliary tract, stomach, skin, salivary gland, head and neck). This study
261 should stimulate investigations in these other cancer types.

262

263 **CONCLUSION**

264 Perineural invasion of cancer cells is associated with angiogenesis and vascular
265 remodeling of vasa nervorum in locally advanced prostate cancer.

266

267 **ACKNOWLEDGMENT**

268 Preliminary portions of this work have been presented elsewhere³¹.

269
270 **CONFLICT OF INTEREST**

271 None

272
273 **ORCID**

274 *Nicolae Ghinea* iD <http://orcid.org/0000-0002-7994-6346>

275
276 ***Author Contributions:***

277 *Study concept and design:* Ghinea

278 *Acquisition of data:* Robin, Leclere, Nicolas

279 *Analysis and interpretation of data:* Robin, Leclere, Nicolas, Pichon, Chnecker, Côté,
280 Guillonneau, Radu, Ghinea

281 *Drafting of the manuscript:* Ghinea, Radu

282 *Critical revision of the manuscript for important intellectual content:* Robin, Leclere,
283 Nicolas, Pichon, Chnecker, Côté, Guillonneau, Radu, Ghinea

284 *Statistical analysis:* Robin, Ghinea

285 *Supervision:* Ghinea, Guillonneau

286 *Other:* None

287
288 **REFERENCES**

- 289 1. Fidler IJ. The pathogenesis of cancer metastasis: the 'seed and soil' hypothesis
290 revisited. *Nat Rev Cancer*. 2003;3:453–8.

- 291 2. Marchesi F, Piemonti L, Mantovani A, Allavena P. Molecular mechanisms of perineural
292 invasion, a forgotten pathway of dissemination and metastasis. *Cytokine Growth Factor*
293 *Rev.* 2010;21:77–82.
- 294 3. Liebig C, Ayala G, Wilks JA, Berger DH, Albo D. Perineural invasion in cancer: a review
295 of the literature. *Cancer.* 2009;115:3379–91.
- 296 4. Batsakis JG. Nerves and neurotropic carcinomas. *Ann Otol Rhinol Laryngol.*
297 1985;94:426–7.
- 298 5. Batchelor PE, Liberatore GT, Wong JY, Porritt MJ, Frerichs F, Donnan GA, Howells DW.
299 Activated macrophages and microglia induce dopaminergic sprouting in the injured
300 striatum and express brain-derived neurotrophic factor and glial cell line-derived
301 neurotrophic factor. *J Neurosci.* 1999;19:1708–16.
- 302 6. Scaloni CS, Banerjee R, Inglehart RC, et al. Galanin modulates the neural niche to favor
303 perineural invasion in head and neck cancer. *Nat Commun.* 2015;6:6885.
- 304 7. Bakst RL, Lee N, He S, Chernichenko N, Chen CH, Linkov G, Le HC, Koutcher J, Vakiani
305 E, Wong RJ. Radiation impairs perineural invasion by modulating the nerve
306 microenvironment. *PLoS One.* 2012;7:e39925.
- 307 8. Amit M, Na'ara S, Gil Z. Mechanisms of cancer dissemination along nerves. *Nat Rev*
308 *Cancer.* 2016;16:399-408.
- 309 9. Li R, Wheeler T, Dai H, Ayala G. Neural cell adhesion molecule is upregulated in nerves
310 with prostate cancer invasion. *Hum Pathol.* 2003;34:457–61.
- 311 10. Ayala GE, Dai H, Ittmann M, Li R, Powell M, Frolov A, et al. Growth and survival
312 mechanisms associated with perineural invasion in prostate cancer. *Cancer Res.*
313 2004;64:6082–6090.
- 314 11. Ayala GE, Dai H, Powell M, et al. Cancer-related axogenesis and neurogenesis in
315 prostate cancer. *Clin Cancer Res.* 2008;14:7614–23.
- 316 12. Fromont G, Godet J, Pires C, Yacoub M, Dore B, Irani J. Biological significance of
317 perineural invasion (PNI) in prostate cancer. *The Prostate.* 2012;72:542–8.

- 318 13. Zhang Y, Toneri M, Ma H, Yang Z, Bouvet M, Goto Y, Seki N, Hoffman RM. Real-Time
319 GFP intravital imaging of the differences in cellular and angiogenic behavior of
320 subcutaneous and orthotopic nude-mouse models of human PC-3 prostate cancer. *J Cell*
321 *Biochem.* 2016;117:2546–51.
- 322 14. Green FL, Compton CC, Fritz AG, Shah JP, Winchester DP, eds. American Joint
323 Committee on Cancer: AJCC cancer staging atlas. Heidelberg, Germany: Springer-
324 Verlag, 2006.
- 325 15. Heidenreich A, Böhmer D. Multimodal therapy of locally advanced prostate cancer. *Der*
326 *Urologe.* 2016;55:333–44.
- 327 16. Eble JN, Sauter G, Epstein JI, Sesterhenn IA, eds. World Health Organization
328 classification of tumours: pathology and genetics of tumours of the urinary system and
329 male genital organs. Lyon, France IARC Press, 2004.
- 330 17. Planeix F, Siraj MA, Bidard F-C, Robin B, Pichon C, Sastre-Garau X, Antoine M, Ghinea
331 N. Endothelial follicle-stimulating hormone receptor expression in invasive breast cancer
332 and vascular remodeling at tumor periphery. *J Exp Clin Cancer Res.* 2015;34:12. DOI
333 10.1186/s13046-015-0128–7.
- 334 18. Powell MS, Li R, Dai H, Sayeeduddin M, Wheeler TM, Ayala GE. Neuroanatomy of the
335 normal prostate. *The Prostate.* 2005;65:52–7.
- 336 19. De Brot S, Ntekim A, Cardenas R, et al. Regulation of vascular endothelial growth factor
337 in prostate cancer. *Endocr Relat Cancer.* 2015;22:R107-23.
- 338 20. Reddy CL, Yosef N, Ubogu EE. VEGF-A165 potently induces human blood-nerve barrier
339 endothelial cell proliferation, angiogenesis and healing *in vitro.* *Cell Mol*
340 *Neurobiol.* 2013;33:789-801.
- 341 21. Bettencourt MC, Bauer JJ, Sesterhenn IA, Connelly RR, Moul JW. CD34
342 immunohistochemical assessment of angiogenesis as a prognostic marker for prostate
343 cancer recurrence after radical prostatectomy. *J Urol.* 1998;160:459–65.

- 344 22. Miyata Y, Sakai H. Reconsideration of the clinical and histopathological significance of
345 angiogenesis in prostate cancer: Usefulness and limitations of microvessel density
346 measurement. *Int J Urol*. 2015;806-15.
- 347 23. Radu A, Pichon C, Camparo P, et al. Expression of follicle-stimulating hormone receptor
348 in tumor blood vessels. *N Engl J Med*. 2010;363:1621-30.
- 349 24. Calzà L, Giardino L, Giuliani A, Aloe L, Levi-Montalcini R. Nerve growth factor control of
350 neuronal expression of angiogenic and vasoactive factors. *Proc Natl Acad Sci U S A*.
351 2001;98:4160–5.
- 352 25. Nico B, Mangieri D, Benagiano V, Crivellato E, Ribatti D. Nerve growth factor as an
353 angiogenic factor. *Microvasc Res*. 2008;75:135–41.
- 354 26. Zahalka AH, Arnal-Estapé A, Maryanovich M, et al. Adrenergic nerves activate an angio-
355 metabolic switch in prostate cancer. *Science*. 2017;358:321–6.
- 356 27. Aragon-Ching JB, Madan RA, Dahut WL. Angiogenesis inhibition in prostate cancer:
357 current uses and future promises. *J Oncol*. 2010;2010:361836. doi:
358 10.1155/2010/361836.
- 359 28. Bergers G, Hanahan D. Modes of resistance to anti-angiogenic therapy. *Nat Rev Cancer*.
360 2008;8:592–603.
- 361 29. Ejaz S, Chekarova I, Ejaz A, Sohail A, Lim CW. Importance of pericytes and mechanisms
362 of pericyte loss during diabetes retinopathy. *Diabetes Obes Metab*. 2008;10:53-63.
- 363 30. Dahl-Jørgensen K. Diabetic microangiopathy. *Acta Paediatr Suppl*. 1998; 425:31-4.
- 364 31. Ghinea N. Angiogenesis and vascular remodeling of vasa nervorum in locally advanced
365 prostate cancer. *J Clin Oncol*. DOI: 10.1200/JCO.2018.36.6_suppl.341.

367 **FIGURE LEGENDS**

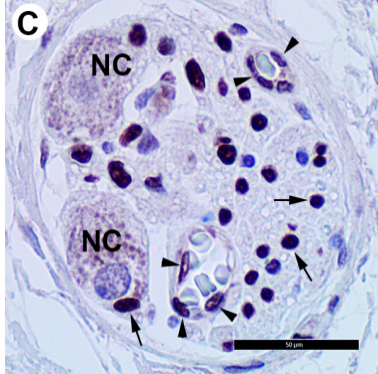
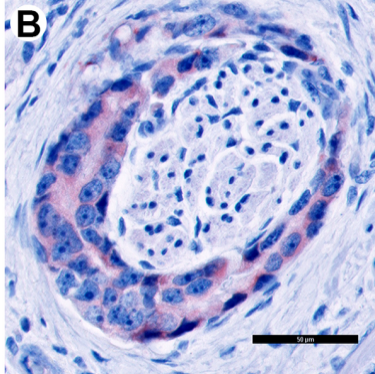
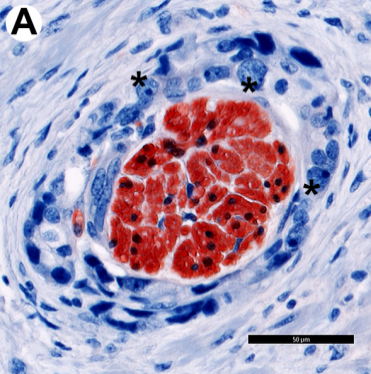
368 **FIGURE 1. Prostate cancer cells that left the primary tumor site are visible along**
369 **nerves.** Immunohistochemical analysis was performed on paraffin-embedded sections of

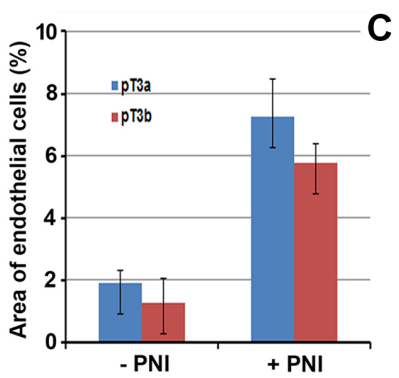
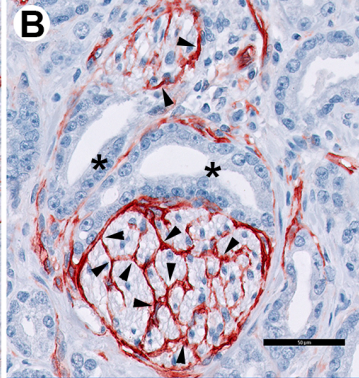
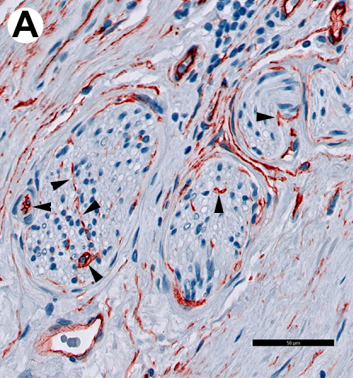
370 human prostate cancer tissues using as primary antibodies a rabbit polyclonal antibody
371 against S100 (a nerve marker), a rabbit polyclonal antibody against VEGF, and a mouse
372 monoclonal antibody against FGF-2. Panel A: Nerve fibers (red color) surrounded by
373 cancerous prostatic glands (asterisks). Panel B: Epithelial cancer cells (red-brown color)
374 expressing VEGF. Panel C: Vasa nervorum endothelial cells (arrowheads) and Schwann
375 cells (arrows) expressing FGF-2 (brown color). NC, nerve cells. Bars: 50 μ m.
376

377 **FIGURE 2. Expression of CD34 by vasa nervorum endothelial cells in locally**
378 **advanced prostate cancer.** Immunohistochemical analysis was performed on paraffin-
379 embedded sections of prostate tumors using the monoclonal antibody CD34 followed by
380 a secondary peroxidase-coupled goat anti-mouse immunoglobulin visualized by the red-
381 brown peroxidase-reaction product of aminoethyl-carbazole. Sections were also stained
382 with hematoxylin. Vasa nervorum (arrowheads) of prostatic nerves without perineural
383 invasion (panel A) showed faint CD34 staining, whereas a strong presence of CD34 was
384 noticed on vasa nervorum of prostatic nerves with perineural invasion (panel B).
385 Asterisks: cancerous glands. Bars: 50 μ m. Panel C: quantitation of CD34-positive vasa
386 nervorum endothelial cells in nerves with perineural invasion (+PNI) or without perineural
387 invasion (-PNI). No differences are noticed between the pT3a (blue bars) and pT3b
388 tumors (red bars).
389

390 **FIGURE 3. Vasa nervorum remodeling in patients diagnosed with locally advanced**
391 **prostate cancer.** Standard histochemical methods with haematoxylin-eosin-saffron
392 staining of cell inclusions and nuclei (panels A and B), periodic acid-Schiff reaction for
393 glycogen, glycoproteins, glycolipids, and proteoglycans (panel C), and Masson's
394 trichrome technique for collagen (panel D). In 22% of patients the subendothelial layer
395 (asterisks) of vasa nervorum contains collagen fibers and is characterized by the
396 absence of pericytes. For most vasa nervorum (panel B) the intima consists of

397 endothelial cells and their basal membrane. In context of cancer, the vasa nervorum
398 endothelial cells (arrows) and Schwann cells (arrowheads) of prostatic nerve ganglions
399 showed strong presence of FSHR (panel E and inset i1). L, capillary lumen; NC, nerve
400 cells; Bars: 50 μm .





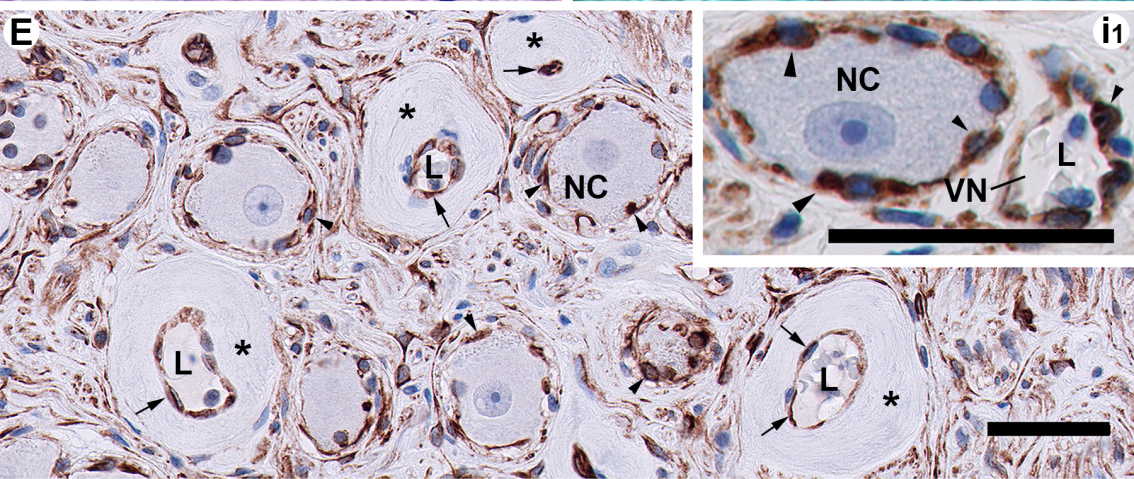
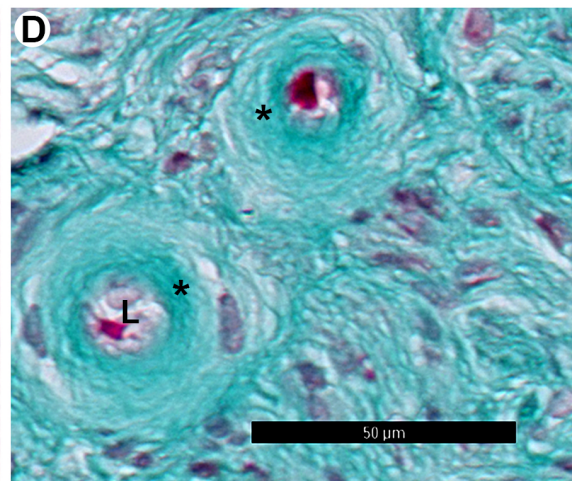
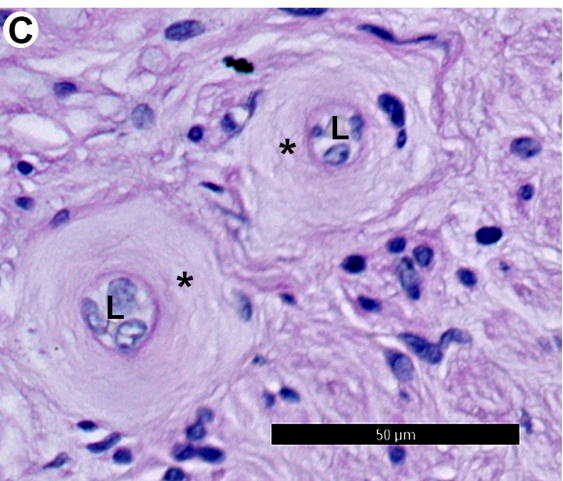
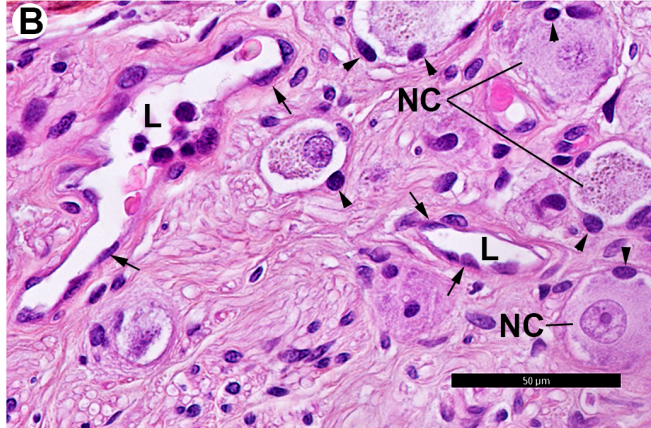
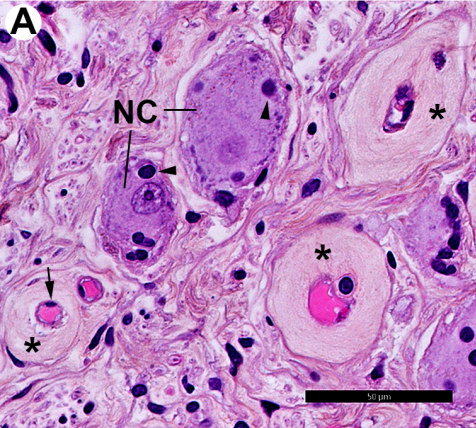


TABLE 1. Clinical characteristics of the study patients

Clinical characteristics of patients	All cases (n = 85)	pT3a (n = 70)	pT3b (n = 15)
Age at prostatectomy [median (range)]	67.3 (58 - 78)	68 (58 - 78)	67 (62 -70)
PSA at diagnosis [median (range)]	7.3 (3.6 - 26)	7 (3.6 - 26)	7.4 (6 - 18.6)
Gleason score			
< 7	22	17	5
≥ 7	63	53	10
Seminal vesicle extension			
No	70	70	0
Yes	15	0	15

TABLE 2. Primary antibodies used in present the immunohistochemical present study

Antibody	Specificity	Description	Isotype	Antigen retrieval	Incubation time	Dilution	Supplier
Qbend-10	CD34	mouse monoclonal	IgG1	Tris-EDTA pH9	30 min	1/200	DAKO
RB-9031	VEGF	rabbit polyclonal		Citrate pH6	60 min	1/100	Thermo / LabVision
11B55	VEGFR-2	rabbit polyclonal		Tris EDTA pH9	60 min	1/100	Cell Signaling
bFM-2	FGF-2	mouse monoclonal	IgG1	Citrate pH6	30 min	1/100	MERCK
D2-40	Podoplanin	mouse monoclonal	IgG1	Citrate pH6	30 min	1/500	DAKO
S-2644	S100	rabbit polyclonal		Citrate pH6	30 min	1/3000	Sigma
FSHRA02	FSHR	mouse monoclonal	IgG2a	Citrate pH6	30 min	50 ng/ml	Institut Curie